

# Reversible Ionic Aggregation Kinetics in Concentrated Electrolytes

Zachary A. H. Goodwin\*

*John A. Paulson School of Engineering and Applied Sciences,  
Harvard University, Cambridge, Massachusetts 02138, United States and  
Department of Materials, University of Oxford, Parks Road, Oxford OX1 3PH, United Kingdom  
(Dated: March 10, 2026)*

Here we develop and test a formalism for reversible ionic aggregation kinetics in an example concentrated electrolyte. Specifically, building on previous equilibrium work of McEldrew and co-workers in the context of concentrated electrolytes, and non-equilibrium properties of thermoreversible polymers and patchy particle systems, we develop the formalism for how ionic associations in electrolytes change subject to a step-change in conditions. This is achieved through solving a macroscopic rate equation of open/occupied association sites, which is a solution of the reversible Smoluchowski aggregation equation. We compare the derived equations against atomistic molecular dynamics simulations of a salt-in-ionic liquid. Good qualitative agreement is obtained, but quantitative differences are found, which highlights the multiple time scales of the associations that exist in concentrated electrolytes. We hope this formalism acts as the starting point for investigating these properties in other electrolytes, and developing it further to investigate the non-Newtonian behaviour of concentrated electrolytes, double layer charging, and the slow dynamics of these electrolytes in confinement.

## I. INTRODUCTION

Concentrated electrolytes, such as water-in-salt electrolytes (WiSES) [1–7], ionic liquids (ILs) [8–11], salt-in-ILs (SiILs) [12–15], amongst many other examples, are increasingly of interest in various applications [9–11, 16–23]. For example, ILs have potential applications as ‘green’ solvents for electrochemical reactions at electrified interfaces, and electrolytes for supercapacitors owing to their low vapour pressure and flammability, and because of their wide electrochemical stability window (ESW) [8–11]. Similarly, WiSEs are promising alternative electrolytes for batteries which are non-flammable, owing to water being the solvent, but still have a wide ESW owing to the high salt concentration [24–27]. Finally, SiILs, or salt-doped ILs, are also finding applications in energy applications, where the unique properties of ILs are being exploited as the solvent to dissolve active cations for intercalation into electrodes [28–30].

These electrolytes also pose interesting fundamental questions, which have advanced our understanding of these correlated systems [21, 31, 32]. For example, in ILs [33–35], and also other electrolytes (WiSEs [36, 37] and SiILs [15]), the observation of “anomalous under-screening” raised questions about extremely long-ranged force decay lengths from bulk, equilibrium electrostatics [38, 39]. While recent research has indicated these are non-equilibrium measurements [40], this motivated much work into understanding concentrated electrolytes [41–46]. Furthermore, WiSEs behave in a non-Newtonian way [47], and have nano-channels of ionic aggregates interpenetrated by water domains for facile transport of the active cations [24–27]. In the context of SiILs, negative transference numbers of alkali metal cations gener-

ated much interest in studying the transport properties of concentrated electrolytes [12, 13].

Much of these properties have been understood, at least in part, from the ionic aggregates and solvation environments that exist in the electrolytes [21, 31, 32, 48]. For example, the negative transference numbers of SiILs can be explained through the formation of a negative shell of anions around the alkali metal cations [12, 13]. Moreover, more generally, ionic associations and solvation is known to be important in understanding inter-phase formation in batteries [49–51], the kinetics of electrocatalysis reactions [20], etc. Typically, these observations have been from the first solvation shell, i.e., through the coordination environments of the electrolytes, and computing the relative numbers of solvent separated ion pairs, contact ion pairs and aggregates. Such approaches, however, provide little fundamental insight into the underlying laws which link these coordination environments to other properties of the electrolytes.

There are, however, microscopic theories which directly link the ionic association and solvation to physicochemical properties of these electrolytes [52, 53]. A notable example is the thermoreversible ionic aggregation model developed by McEldrew *et al.* [53–58], which links coordination environments to activity [23], transference numbers, electrical double layers [59–62] and many more properties. This theory is founded on the classical polymer theories of Flory, Stockmayer and Tanaka [63–74], which describe the thermoreversible association of monomer units into a polymer, where McEldrew *et al.* [53] translated this to the thermoreversible association of ions into aggregates (or an alternating copolymer of cations and anions, decorated by solvent). This system of equations [75–77] has also been actively used to understand the phase and fluid behavior of patchy particle systems [78, 79].

While McEldrew *et al.* have mainly investigated equi-

\* zac.goodwin@materials.ox.ac.uk

librium and linear-response transport properties [53, 55–57], in the context of polymers and patchy particle systems, various non-equilibrium properties have been investigated. For example, Sciortino, Tartaglia and co-workers connected the kinetics of patchy particle aggregation to the distribution of clusters [75–77, 80–84], and the viscous and elastic response of polymers with thermoreversible associations was recently studied by Tanaka [85, 86]. This presents itself as a significant gap in the literature, where concentrated electrolytes could greatly benefit from further drawing on these fields of research. For example, the dynamics of ionic associations are routinely studied (through residence times) of electrolytes [12, 13], and it is known that the desolvation time scale is important for intercalation rates [87]. However, more quantitatively linking these to a microscopic theory remains lacking [88].

Here, we take the first steps to apply the non-equilibrium formalisms from polymer and patchy particle systems to concentrated electrolytes. Specifically, we investigate the dynamics of reversible ionic aggregation in a bulk SiIL. First we present an overview of the formalism in the bulk at equilibrium, before extending it to non-equilibrium conditions, building upon previous work in patchy particle systems. Next, we outline and perform classical molecular dynamics simulations to test the derived equations. Overall, qualitative agreement is found between theory and simulations. The quantitative differences between the theory and simulations reveal a fundamental limitation of the assumed equations. That being, a single rate constant can describe the ionic aggregation over all time scales. Whereas, in the simulations we find multiple time scales. Overall, the formalism provides insight into the kinetics of reversible ionic aggregation in SiILs, hints at further developments of the theory, demonstrates the multi-time-scale nature of concentrated electrolytes, and provides a starting framework to further investigate kinetics in various aspects of concentration electrolytes and linking it to the coordination environments.

## II. THEORY

Here we study salt-in-ionic liquids (SiILs) as an example system to investigate the kinetics of ionic aggregation. In particular, we study alkali metal doped ILs, where the anion is the same in each salt (3 species in total). These have been studied for a while, owing to their promise in energy storage systems, and the observed negative transference number of the alkali metal cation at low alkali metal doping levels [12, 13]. Previously, McEldrew *et al.* developed an equilibrium theory of the bulk ionic aggregates [56], quantified the effective charge of the alkali metal cation, and studied the electrical double layer [15, 62]. We recommend that the reader familiarities themselves with these previous works [15, 56, 62], also for other electrolytes [23, 55, 57, 58], since the for-

malism has a significant learning curve. Nonetheless, we provide a brief summary of the equilibrium theory before progressing onto the kinetics of aggregate formation.

From the electrolytes that have studied with this formalism so far, SiILs is one of the most challenging [56]. Its concentrated and correlated nature pushes the boundaries of the theory [15], where loops within the aggregates form (breaking the Cayley tree approximation), making it more difficult to apply the theory. While SiILs are the most challenging example that have been applied this theory to so far, we nonetheless use it as a test case. In future work, applied to other electrolytes, we expect the developed formalism to perform even better.

### A. Equilibrium Theory Overview

The alkali metal cations and anions are assumed to form a polydisperse mixture of Cayley-tree aggregates (see Refs. 53, 56 for justification) through the associations in their first coordination shell, which can form a percolating ionic network, also called the gel phase [53, 56]. The IL cations are assumed not to participate in ionic associations directly, but can still influence the aggregates through interacting with the anion (see Refs. 56, 89). This is schematically shown in Fig. 1.

We treat the SiIL as an incompressible lattice fluid [53, 56]. The alkali metal cations are denoted by  $+$ , and IL cations denoted by  $\oplus$ , and anions by  $-$ . The total volume fractions of ions,  $\phi_j$ , are known, with  $1 = \phi_+ + \phi_- + \phi_{\oplus}$  from the incompressibility constraint. The lattice site is assumed to be the volume of the alkali metal cation,  $v_+$ . The volumes occupied by the other ions are expressed relative to this volume through  $v_+\xi_j$ , where  $\xi_j = v_j/v_+$ . The (dimensionless) concentration of each ion per lattice site is given by  $c_j = \phi_j/\xi_j$  [53, 56].

The alkali metal cations can form a maximum of  $f_+$  associations, and the anions a maximum of  $f_-$  associations. This is referred to as the functionality [53, 56]. As these functionalities are larger than 1, a polydisperse cluster distribution can form with clusters of rank  $lm$ , where  $l$  is the number of cations and  $m$  is the number of anions, with dimensionless concentration  $c_{lm}$  [53, 56]. For functionalities equal to or larger than 2, a percolating ionic network can emerge [53]. This is referred to as the gel here. In the gel regime, we employ Flory's convention to determine the volume fractions of ions in the sol ( $\phi_{+/-}^{sol}$ , i.e., not the gel phase) and gel phase ( $\phi_{+/-}^{gel}$ ), where  $\phi_{+/-} = \phi_{+/-}^{sol} + \phi_{+/-}^{gel}$ . The total dimensionless concentration of alkali metal cations is given  $c_+ = \sum_{lm} l c_{lm} + c_+^{gel}$  and anions  $c_- = \sum_{lm} m c_{lm} + c_-^{gel}$ . Note  $\phi_{lm} = (l + \xi_- m) \bar{c}_{lm}$  also helps convert between volume fractions and dimensionless concentrations.

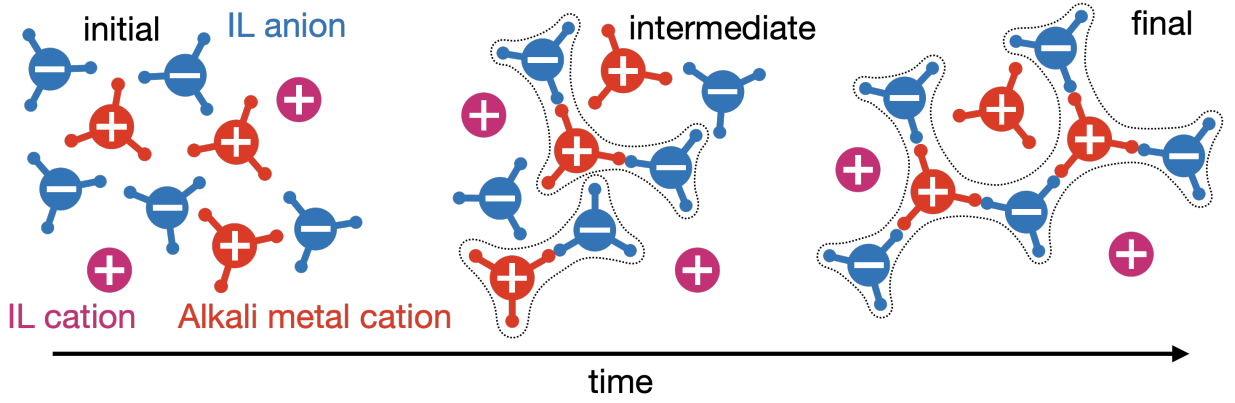


FIG. 1. Schematic of non-equilibrium kinetics of ionic aggregation in the studied salt-in-ionic liquid (SIIL). The alkali metal cation and IL anion bind together to form aggregates. From step-changing a property of the system, we investigate how they evolve in time. The alkali metal cation and IL anions are shown with 3 dangling bonds, to represent they can form associations, while the IL cations are shown without, since they do not associate strongly with the anions.

The free energy functional [15, 53, 56, 62] is given by

$$\begin{aligned}
v_+ \mathcal{F} = & \int_V d\mathbf{r} \frac{c_{\oplus}}{\beta} \ln \phi_{\oplus} + \sum_{lm} \left( \frac{c_{lm}}{\beta} \ln \phi_{lm} + c_{lm} \Delta_{lm} \right) \\
& + \int_V d\mathbf{r} \chi \phi_{\oplus} \sum_{lm} (f_- m - m - l + 1) c_{lm} \\
& + \int_V d\mathbf{r} \left( \Delta_+^{gel} c_+^{gel} + \Delta_-^{gel} c_-^{gel} \right), \quad (1)
\end{aligned}$$

where  $\beta^{-1} = k_B T$  is inverse thermal energy. The first term is the ideal entropy of the IL cations, and the second term is the ideal entropy from all clusters. The third term is the free energy of forming clusters, where  $\Delta_{lm}$  is the free energy of forming each cluster of rank  $lm$ . The fourth term is the regular solution interaction between the IL cations and open anion binding sites (see Refs. 15, 56, 62), with strength  $\chi$ . The fifth term comes from the free energy of ions associating to the gel,  $\Delta_j^{gel}$ .

The chemical potential of a rank  $lm$  cluster,  $\mu_{lm}$ , can be determined by differentiating the free energy with respect to  $c_{lm}$ . Establishing equilibrium between clusters of rank  $lm$  and their free counterparts, we have

$$\mu_{lm} = l\mu_{10} + m\mu_{01}. \quad (2)$$

Using the chemical potential expressions, we obtain the cluster equilibrium

$$\phi_{lm} = K_{lm} \phi_{10}^l \phi_{01}^m, \quad (3)$$

where  $K_{lm} = \exp \{ (l+m-1)(1+\beta\chi\phi_{c_1}) - \beta\Delta_{lm} \}$  is the equilibrium constant. We consider the free energy of forming a cluster of rank  $lm$ ,  $\Delta_{lm}$ , to have three contributions

$$\Delta_{lm} = \Delta_{lm}^{comb} + \Delta_{lm}^{conf} + \Delta_{lm}^{bind}, \quad (4)$$

where  $\Delta_{lm}^{comb}$  is the combinatorial entropy,  $\Delta_{lm}^{conf}$  is the configurational entropy and  $\Delta_{lm}^{bind}$  is the binding energy. The combinatorial entropy is given by

$$\Delta_{lm}^{comb} = -\frac{1}{\beta} \ln f_+^l f_-^m W_{lm}, \quad (5)$$

where  $W_{lm}$  is the enumeration of the ways that a rank  $lm$  cluster can be formed. For Cayley trees, Stockmayer [64–66] determined the expression to be

$$W_{lm} = \frac{(f_+ l - l)!(f_- m - m)!}{l! m! (f_+ l - l - m + 1)!(f_- m - m - l + 1)!}. \quad (6)$$

The binding energy is approximated as the energy of a single association,  $\Delta u$ , multiplied by the total number of associations in a cluster, which for Cayley tree clusters is  $l+m-1$ . Thus, the binding energy is

$$\Delta_{lm}^{bind} = (l+m-1)\Delta u. \quad (7)$$

The configurational entropy describes the entropy of placing a rank  $lm$  cluster on the lattice. We modify Flory's expression [53], for the so-called entropy of disorientation [63, 68, 73, 90], to be

$$\beta \Delta_{lm}^{conf} = -\ln \left( \frac{l + \xi_- m}{\xi_-^m} \right) - (l+m-1)(\beta T \Delta s - 1), \quad (8)$$

where  $\Delta s$  is a per-association entropy change [23].

From using  $\Delta_{lm}$ , we obtain the thermodynamically consistent cluster distribution

$$c_{lm} = \frac{W_{lm}}{\lambda} (\lambda f_+ \phi_{10})^l (\lambda f_- \phi_{01} / \xi_-)^m, \quad (9)$$

where  $\lambda$  is the association constant given by

$$\lambda = \exp \{ \beta (-\Delta u + T\Delta s + \chi\phi_{\oplus}) \}. \quad (10)$$

In Eq. (9),  $c_{lm}$  is written in terms of the volume fraction of free alkali metal cations ( $\phi_{10}$ ) and anions ( $\phi_{01}$ ). These quantities are, however, not *a priori* known, and moreover, we aimed to predict them from the theory, not have them as inputs for it. To overcome this, we [53, 56, 67–74] express  $\phi_{10/01}$  in terms of  $\phi_{+/-}$  and introduce ion association probabilities,  $p_{ij}$ , which is the probability that an association site of species  $i$  is bound to species  $j$ . Therefore, the volume fraction of free alkali cations can be written as  $\phi_{10} = \phi_{+}(1 - p_{+-})^{f_{+}}$  and free anions as  $\phi_{01} = \phi_{-}(1 - p_{-+})^{f_{-}}$ .

The association probabilities can be determined through the mass action law

$$\lambda\zeta = \frac{p_{+-}p_{-+}}{(1 - p_{+-})(1 - p_{-+})}, \quad (11)$$

and conservation of associations

$$p_{+-}\psi_{+} = p_{-+}\psi_{-} = \zeta, \quad (12)$$

where  $\psi_{+/-} = f_{+/-}\phi_{+/-}/\xi_{+/-}$  is the total dimensionless concentration of association sites (per lattice) [53, 56]. Equations (12) and (11) permit an explicit solution for the probabilities

$$\lambda\zeta = \frac{1 + \lambda\psi_{\pm} - \sqrt{[1 + \lambda\psi_{\pm}]^2 - 4\lambda^2\psi_{+}\psi_{-}}}{2}. \quad (13)$$

where  $\psi_{\pm} = \psi_{+} + \psi_{-}$ . It has been shown, from a bond percolation analysis, that the percolating ionic network onsets when  $p_{+-}p_{-+} = 1/(f_{+} - 1)/(f_{-} - 1)$ , which we also call the gel-point (see Refs. 53, 56). To determine sol and gel properties in the post-gel regime, we use Flory's treatment [53].

## B. Reversible Aggregation Kinetics

Next we outline the non-equilibrium theory for reversible ionic aggregation kinetics in bulk SiLLs. This has not been explored in the context of concentrated electrolytes before. However, in the context of patchy-particle systems, an ostensibly similar system, the kinetics of aggregation has been well studied [75, 77, 80–84]. In this section, the presented formalism closely follows to the works of Sciortino, Tartaglia and co-workers [75, 77, 80–84], and Dongen and Ernst [91].

The reversible Smoluchowski equation governs the time evolution of thermoreversible aggregation. This master equation describes how the change in concentration of an aggregate of rank  $lm$ , in the two-component

case studied here, with concentration  $c_{lm}(t)$ , depends on the rates of formation and destruction of this aggregate

$$c_{l-l',m-m'} + c_{l',m'} \xrightleftharpoons[F_{l',l',m,m'}^{(f)}]{K_{l,l',m,m'}^{(f)}} c_{l,m}, \quad (14)$$

$$c_{l,m} + c_{l',m'} \xrightleftharpoons[F_{l,l',m,m'}^{(r)}]{K_{l,l',m,m'}^{(r)}} c_{l+l',m+m'}. \quad (15)$$

The first reversible aggregation reaction, Eq. (14), describes the rate of formation of  $c_{l,m}$  through the binding between  $c_{l-l',m-m'}$  and  $c_{l',m'}$  with a rate of  $K_{l,l',m,m'}^{(f)}$  [84, 91]. Note we have left the rate constant to generally depend on the values of  $l, l', m$  and  $m'$ , with exactly how the rate depends on these values being shown later, and explicitly use the concentrations of these ranks of clusters. In this same equilibrium,  $c_{l,m}$  can be removed through breaking an association to form  $c_{l-l',m-m'}$  and  $c_{l',m'}$  with rate  $F_{l',l',m,m'}^{(f)}$ . While the second reversible aggregation reaction, Eq. (15), describes the removal of  $c_{l,m}$  through the formation of an association with  $c_{l',m'}$  to form  $c_{l+l',m+m'}$ , with a rate of  $K_{l,l',m,m'}^{(r)}$ , again generally given. In addition, there is the formation of  $c_{l,m}$  from the dissociation of  $c_{l+l',m+m'}$ , with rate  $F_{l,l',m,m'}^{(r)}$  [84, 91]. These reversible aggregation reactions can be seen in the reversible Smoluchowski aggregation equation

$$\begin{aligned} \frac{dc_{lm}}{dt} = & \sum_{\substack{l'=0, \\ m'=0}}^{\infty} \left( c_{l+l',m+m'} F^{(r)} - c_{lm} c_{l',m'} K^{(r)} \right), \\ & + \frac{1}{2} \sum_{\substack{l'+l''=l, \\ m'+m''=m}} \left( c_{l'm'} c_{l''m''} K^{(f)} - c_{l,m} F^{(f)} \right) \end{aligned} \quad (16)$$

where the subscripts of  $K_{l,l',m,m'}^{(f/r)}$  and  $F_{l,l',m,m'}^{(f/r)}$  were dropped for clarity, and the explicit time-dependence of the concentrations suppressed [84].

As discussed in detail in Refs. 84, 91, the rates of fragmentation ( $F$ ) and coalescence ( $K$ ) depend on the time-scale for an association to form and the diffusive time-scales of the species which associate. The total rates of fragmentation and coalescence depend on both of these time-scales. There are, of course, different limiting cases, where the kinetics can be diffusion controlled or reaction (association) controlled [84].

At equilibrium ( $t = \infty$ ), the steady state solution of Eq. (15) imposes [84]

$$c_{l,m}(\infty) c_{l',m'}(\infty) K^{(r)} = F c_{l+l',m+m'}(\infty). \quad (17)$$

Moreover, we can introduce the elementary rates for the formation of a single association,  $k$ , and the rate of a single dissociation,  $f$ , which is related to the (equilibrium)

association constant through  $\lambda = k/f$  [84, 91]. In the  $RA_f$  model, the coalescence rate for two aggregates is related to the number of dangling association sites in each aggregate, since all dangling association sites are equally reactive [84, 91]. For a cluster of rank  $lm$ , this is

$$\sigma_{lm} = (f_+l - l - m + 1)!(f_-m - m - l + 1)!, \quad (18)$$

which then relates the full coalescence rate to the rate of an individual association formation

$$K_{l,l',m,m'}^{(r)} = k\sigma_{lm}\sigma_{l'm'}. \quad (19)$$

Therefore, from Eq. (17), the full fragmentation rate is related to the rate of an individual fragmentation through

$$F_{l,l',m,m'}^{(r)} = f\sigma_{lm}\sigma_{l'm'} \frac{W_{lm}W_{l'm'}}{W_{l+l',m+m'}}. \quad (20)$$

The same procedure can be repeated for Eq. (14), although not shown here [84, 91].

In principle, this determines the reversible Smoluchowski aggregation equation to be solved [84, 91]. Directly solving the reversible Smoluchowski aggregation equation is a formidable task, however. Even in the irreversible Smoluchowski equation, direct solutions are limited to, for example, simple initial conditions (monomers only) and certain choices of the rate kernels ( $K$  and  $F$ ). However, Flory and Stockmayer, and later others, demonstrated that the association probabilities could be used as the central variable, greatly simplifying the problem [84, 91]. Instead, the time dependence of the association probabilities is solved for, considering the addition and removal of single associations through this ensemble averaged quantity. It was shown that these time-dependent association probabilities used in the equilibrium cluster distribution, Eq. (9), were a solution of the reversible Smoluchowski aggregation equation, in a quasi-equilibrium way [84, 91]. In what follows, we solve the time-dependence of the association probabilities under different approximations. Again, these solutions closely follow the works of Refs. 84, 91 and the reader is encouraged to familiarize themselves with those works.

### C. Symmetric case

Typically, the functionalities of the alkali metal cation and anion are different in SiILs, which generally means their association probabilities are not equal [56]. However, if the association probabilities to be equal, we must have  $\psi_+ = \psi_-$  (conservation of associations), which can (sometimes) be achieved at a specific composition in SiILs. Since  $f_+ = 4$  typically and  $f_- = 3$  [15], to achieve  $p_{+-} = p_{-+}$ , there must be 3/4 times the number of alkali metal cations as anions. In this section, we con-

sider  $p_{+-} = p_{-+} = p$  generally and do not specify exact values of  $f_i$  or  $\phi_i$  explicitly, other than they satisfy  $\psi_+ = \psi_- = \psi$  to ensure a single association probability.

As demonstrated in Refs. 84, 91, the time-dependence of  $p(t)$  is determined from the macroscopic rate equation

$$\frac{d[A^R]}{dt} = k[A^F]^2 - f[A^R] \quad (21)$$

where  $[A^R] = \psi p$  is the concentrated of bound association sites, and  $[A^F] = \psi(1 - p)$  is the concentration of unbound association sites. The rate of forming a single association,  $k$ , pre-multiplies  $[A^F]^2$ , to obtain the overall rate of forming associations. While the rate of breaking a single association,  $f$ , pre-multiplies  $[A^R]$ , to obtain the overall rate of breaking associations [84, 91]. Similar to the equilibrium theory, this macroscopic rate equation assumes independence and equal reactivities of each association. Thus, the first-order differential which describes the time-dependence of the association probability is given by

$$\frac{1}{k} \frac{dp}{dt} = \psi(1 - p)^2 - \frac{p}{\lambda}. \quad (22)$$

In the SI, we show how this equation can be derived from considering a limiting case of ion pair formation [60]. In the limit of long-time,  $dp(\infty)/dt = 0$ , we find

$$\psi\lambda = \frac{p(\infty)}{[1 - p(\infty)]^2}, \quad (23)$$

which is simply the mass action law, as in Eq. (11), where the conservation of associations has been applied. Since the elemental rates, and therefore, the association constant are determined by the final state, the equilibrium state is naturally incorporated into the differential equation. Before there was a step-change in conditions that results in a variation of the associations, different rate constants and equilibrium constants applied. Upon the step-change, these rates are forgotten, but they initially persist through the initial values of the association probabilities [84, 91].

Applying the initial condition of  $p(0) = p^0$ , we find the solution to be [84, 91]

$$p(t) = \frac{p^\infty(1 - \Lambda e^{-t/\tau})}{1 - p^\infty p^\infty \Lambda e^{-t/\tau}} \quad (24)$$

where  $p(\infty) = p^\infty$  has been introduced, and we have defined the following parameters

$$\Lambda = \frac{p^\infty - p^0}{p^\infty(1 - p^\infty p^0)}, \quad (25)$$

which is a statement of the direction that the association probabilities are changing (if they are increasing or decreasing) and by how much, and

$$\tau^{-1} = \frac{k}{\lambda} \sqrt{[1 + 2\lambda\psi]^2 - 4\lambda^2\psi^2} = k\psi \frac{1 - p^\infty p^\infty}{p^\infty}, \quad (26)$$

is the inverse time-scale that controls the evolution of the association probabilities [84, 91]. We find that this inverse relaxation time depends on two main factors. Firstly, it is proportional to the rate of forming an association [84, 91]. Therefore, different electrolytes could be expected to have different relaxation times, based on this absolute scale, which is information that is removed in the association constant, since that depends on the ratio of the rates [12, 13, 57]. The second term is proportional to a function of the probabilities, which cause a divergent time scale when the association probabilities approach 1. Therefore, in principle, extremely long relaxation times of electrolytes could be obtained from reversible aggregation.

The solution of  $p(t)$ , in Eq. (24), then completely determines the changes in the aggregates in the system, which has been shown to be a solution of the reversible Smoluchowski aggregation equation. Therefore, the aggregates change in a quasi-equilibrium way, i.e., they always have a distribution that obeys an equilibrium cluster distribution [Eq. (9) with the association constant, which changes in time, calculated using the association probabilities], with their changes being completely described through  $p(t)$ . This was noted by Sciortino and co-workers [75, 77, 82] to connect time and temperature through  $p$ , i.e., there is a time in the non-equilibrium aggregation when  $p(t) = p(T)$ , which can be thought to be equivalent to the temperature changing throughout the simulation in.

In the post-gel regime, Eq. (24) still applies, but the total association probabilities can be decomposed into sol and gel contributions, using Flory's post-gel treatment. For more information on how the reversible Smoluchowski aggregation equation is modified, refer to Ref. 91.

We can also study various limits of Eq. (22). An example is irreversible aggregation,  $k \gg f$  and  $\lambda = \infty$ , described by

$$\frac{1}{k} \frac{dp}{dt} = \psi(1 - p)^2. \quad (27)$$

Starting with an initial condition of  $p(0) = 0$ , the solution to this equation is  $p(t) = k\psi t / (1 + k\psi t)$ . This can be seen to be a limit of Eq. (24) from taking  $p(0) = 0$  with  $\lambda \approx \infty$ , i.e.,  $p^\infty \approx 1$ .

If, by contrast, we study irreversible fragmentation, where the initial aggregates can only break apart, we would have

$$\frac{dp}{dt} = -fp. \quad (28)$$

The solution of this is simply  $p(t) = p^0 e^{-ft}$ . Therefore, the aggregates should simply exponentially decay, with

the rate being solely determined by the rate of breaking a single association. This can be seen to be a limit of Eqs. (24)-(26), through taking  $p^\infty$  to be zero and  $\lambda = 0$ . Commonly, the lifetime of associations (residence times) are calculated from MD simulations, and this differential equation would describe it, if there was a single time-scale [12, 92, 93].

#### D. Asymmetric case

Having established the equations for the simplest, symmetric case, in this section we extend the solutions to  $\psi_+ \neq \psi_-$ , referred to as the asymmetric case. Fundamentally, the governing equations are the same form, but the solution is slightly more involved since there are two probabilities,  $p_{+-}$  and  $p_{-+}$ .

As demonstrated in Ref. 91, the time-dependence of the association probabilities is governed by the macroscopic rate equation, give by

$$\frac{d[A^R]}{dt} = k[A^F][B^F] - f[A^R], \quad (29)$$

where  $[B^F]$  is again a concentration of free association sites [91]. Here we take  $A$  to correspond to alkali metal cation sites that can bind to anions, and  $B$  denotes anion sites that can bind to alkali metal cations. Therefore, our governing equation for the change in  $p_{+-}$  is given by [91]

$$\frac{1}{k} \frac{dp_{+-}}{dt} = \psi_-(1 - p_{-+})(1 - p_{+-}) - \frac{p_{+-}}{\lambda}. \quad (30)$$

Clearly, at equilibrium we arrive at

$$\psi_- \lambda = \frac{p_{+-}}{(1 - p_{-+})(1 - p_{+-})}, \quad (31)$$

which is the mass action law of Eq. (11). We can solve Eq. (30), with the initial condition  $p(t=0)_{+-} = p_{+-}^0$ , and arrive at

$$p(t)_{+-} = \frac{p_{+-}^\infty (1 - \Lambda_\pm e^{-t/\tau_\pm})}{1 - p_{+-}^\infty p_{-+}^\infty \Lambda_\pm e^{-t/\tau_\pm}}, \quad (32)$$

where we have defined

$$\Lambda_\pm = \frac{p_{+-}^\infty - p_{+-}^0}{p_{+-}^\infty (1 - p_{-+}^\infty p_{+-}^0)}, \quad (33)$$

and the inverse relaxation time is given by

$$\tau_\pm^{-1} = \frac{k}{\lambda} \sqrt{[1 + \lambda\psi_\pm]^2 - 4\lambda^2\psi_-\psi_+} \quad (34)$$

$$= k\psi_+ \frac{1 - p_{+-} - p_{-+}}{p_{-+}}, \quad (35)$$

This solution is analogous to Eq. (24), and recovers it in the limit of the symmetric case [91].

Equivalently, we could write the counterpart of Eq. (29), and arrive at the governing equation in terms of  $p_{-+}$

$$\frac{1}{K} \frac{dp_{-+}}{dt} = \psi_+(1 - p_{-+})(1 - p_{+-}) - \frac{p_{-+}}{\lambda}, \quad (36)$$

which also recovers the mass action law at equilibrium, and yields, with the initial condition  $p_{-+}^0$ , the following solution

$$p(t)_{-+} = \frac{p_{-+}^\infty(1 - \Lambda_{\mp} e^{-t/\tau_{\pm}})}{1 - p_{-+}^\infty \Lambda_{\mp} e^{-t/\tau_{\pm}}}, \quad (37)$$

where we have defined

$$\Lambda_{\mp} = \frac{p_{-+}^\infty - p_{-+}^0}{p_{-+}^\infty(1 - p_{-+}^\infty)}, \quad (38)$$

with the relaxation time again being given by Eq. (35). Finally, we note that one can convert between Eq. (32) and Eq. (37) through a time-generalized conservation of associations

$$\psi_- p(t)_{-+} = \psi_+ p(t)_{+-}. \quad (39)$$

In the post-gel regime, these equations still apply, but the total association probabilities are decomposed into sol and gel contributions, using Flory's post-gel treatment, as described in the symmetric case [91]. We note that, also as discussed in the symmetric case, we can take limits of irreversible aggregation and fragmentation, where simplified solutions would also be found for the asymmetric case.

### III. MOLECULAR DYNAMICS

To test the equations in the Theory Section, we perform atomistic, classical molecular dynamics simulations of an example SiIL. We choose to study NaTFSI in EMIMTFSI. To perform these simulations, we use LAMMPS [94] and the CL&P force field [95] with charges rescaled by 0.7 to mimic the effect of polarisability [12, 13]. The initial inputs were generated with `fftool` and `packmol` [96]. We studied mole fractions of  $x = 0.25, 0.5, 2/3, 0.75$  in  $\text{NaTFSI}_x\text{EMIMTFSI}_{1-x}$ , with 400 TFSI<sup>-</sup> anions in the simulation cell and varying numbers of each cation. A timestep of 1 fs was utilized, with all hydrogen atoms fixed by shake.

To equilibrate the system, we initially performed a temperature annealing cycle. Starting from a 1 ns run at 300 K (for example), we ramped the system to 450 K over

1 ns, and held at that temperature for another 1 ns, before the same procedure is repeated with a final temperature of 600 K (for higher temperature simulations, e.g., 400 K and 500 K, the same change in temperatures were performed for the annealing cycle). An equivalent cooling cycling was then applied. Then another 10 ns equilibration was performed. This was performed in NPT, where we use a temperature thermostat with 100 fs and 1000 fs for the pressure. In NVT, at the equilibrium density, we then equilibrated for another 10 ns.

To model the effect of the kinetics of aggregation, we need to step-change a property in the simulation. The most natural way of doing this is to step change the temperature. Several simulations were performed, where, for example, we first equilibrated the electrolyte with a density that corresponds to 300 K at a temperature of 500 K, which causes the associations to break from the higher temperature. Then we would step change the temperature back to 300 K, i.e., the temperature of the density that the box is equilibrated to in NVT. This, however, only produces very modest changes in the coordination numbers. The results of these simulations are in the SI, but will be discussed in the main text.

To produce a more substantial effect, to investigate more thoroughly if the kinetic equations derived perform well, we investigated a more artificial test. In MD simulations, we have control over the interactions of the electrolytes. Therefore, we can turn on and off the electrostatic interactions, which is a main driving force for associations in the electrolyte. After the NVT equilibration, as described before, we rescaled all charges by  $10^6$ , making them essentially 0, and equilibrated the electrolyte for 1 ns. Then the original charges (0.7 of the CL&P force field [95]) of the atoms were reinstated, and the changes in coordination numbers tracked in time. Note that turning on and off the charges pumps/removes significant energy into the system. Therefore, while tracking how coordination numbers change in time, we more aggressively thermostated the electrolyte (2 fs for 1000 steps, then 5 fs for 1000 steps, and 10 fs for 1000 steps before the normal value was used for the remainder). This ensured the temperature remained approximately constant (if this was not performed, temperatures in the  $10^3$  K were found). Note we did not find that this aggressive thermostating qualitatively changed the results, with it only resulting in a small quantitative effect.

The association probabilities defined in Eq. (13) are directly linked to the average coordination number of alkali cations by anions ( $f_+ p_{+-}$ ), as well the coordination number of anions by alkali cations ( $f_- p_{-+}$ ). From the MD simulations, we define if a Na<sup>+</sup> and TFSI<sup>-</sup> are associated if the O of TFSI<sup>-</sup> is within 3.3 Å of Na<sup>+</sup>, or vice versa. This was chosen based on the first time  $g(r)$  reaches 1 after the first peak [57], see SI for details. Other real-space cutoffs were investigated too. While the exact quantitative numbers change, the overall conclusions found here remain independent of this choice. Note that if more than 1 O in TFSI<sup>-</sup> is within the cutoff to the same Na<sup>+</sup>

this still just counts as 1 association, i.e., bidendate associations only count as a single association here, as we are counting based on species not functional groups. To determine the ionic aggregates in the simulations, we construct an adjacency matrix to determine the connectivity of the aggregates, which allows the numbers of all aggregates to be computed.

To determine a persistence/residence time (shown in the SI), we use a Heaviside step function between  $\text{Na}^+$  and O in  $\text{TFSI}^-$  to count associations (so  $H(r, t) = 1$  if  $r \geq r_{cut}$  and  $H(r, t) = 0$  if  $r < r_{cut}$ ) to determine an autocorrelation function  $\langle H(r, t)H(r, 0) \rangle$ , which can be used to extract a persistence/residence time [12, 92, 93, 97].

## IV. RESULTS

### A. Symmetric case

In Fig. 2 we show how the coordination numbers between  $\text{Na}^+$  and  $\text{TFSI}^-$  change with time from the non-equilibrium MD simulations, with a comparison against our theory. Here we study the symmetric case of the SiIL  $\text{NaTFSI}_{0.75}\text{EMIMTFSI}_{0.25}$ , since the functionality of  $\text{Na}^+$  is 4 and  $\text{TFSI}^-$  is 3, this electrolyte mixture has  $p_{+-}(t) = p_{-+}(t)$ . Remember, the coordination numbers are related to the probabilities through  $CN_{ij} = f_i p_{ij}$  [56–58]. We choose to show the results in terms of coordination numbers, as these are readily extracted from MD simulations, and it gives distinct numerical values for  $\text{Na}^+$  and  $\text{TFSI}^-$  in this symmetric case. The results for the simulations in Fig. 2 correspond to the charge rescaling case (see Molecular Dynamics Section for further description). In the SI, we show results for the temperature rescaling non-equilibrium conditions. The same conclusions are drawn from those, but where smaller changes in coordination numbers are observed.

Figure 2a) shows the simulations at 300 K. Initially, even though the charges of all atoms are essentially 0, we find coordination numbers of  $\sim 0.3$ . This can be attributed to the fact that a real-space cutoff has been used, and the volume has been constrained to the equilibrium value at 300 K with the normal values of the charge. We find that  $CN_{+-}$  (number of  $\text{TFSI}^-$  anions bound to  $\text{Na}^+$  cations) and  $CN_{-+}$  (number of  $\text{Na}^+$  cations bound to  $\text{TFSI}^-$  anions) initially increases rapidly over the first 2 ps of the simulation, after which they increase less rapidly. After 15 ps, these coordination numbers have *approximately* saturated at their equilibrium values.

To compare against the theory, we have to extract the initial and final association probabilities (which is straightforward). Then the only unknown in the theory is the time-constant of the decay in the probabilities,  $\tau$ , since the rates of forming and breaking associations ( $k$  and  $f$ , respectively) are not known. Using the MD data, we fitted  $CN_{+-/-+}$  over the 17 ps displayed to extract  $\tau$ , which we report in Tab. I. We find that the fitted  $\tau$  for

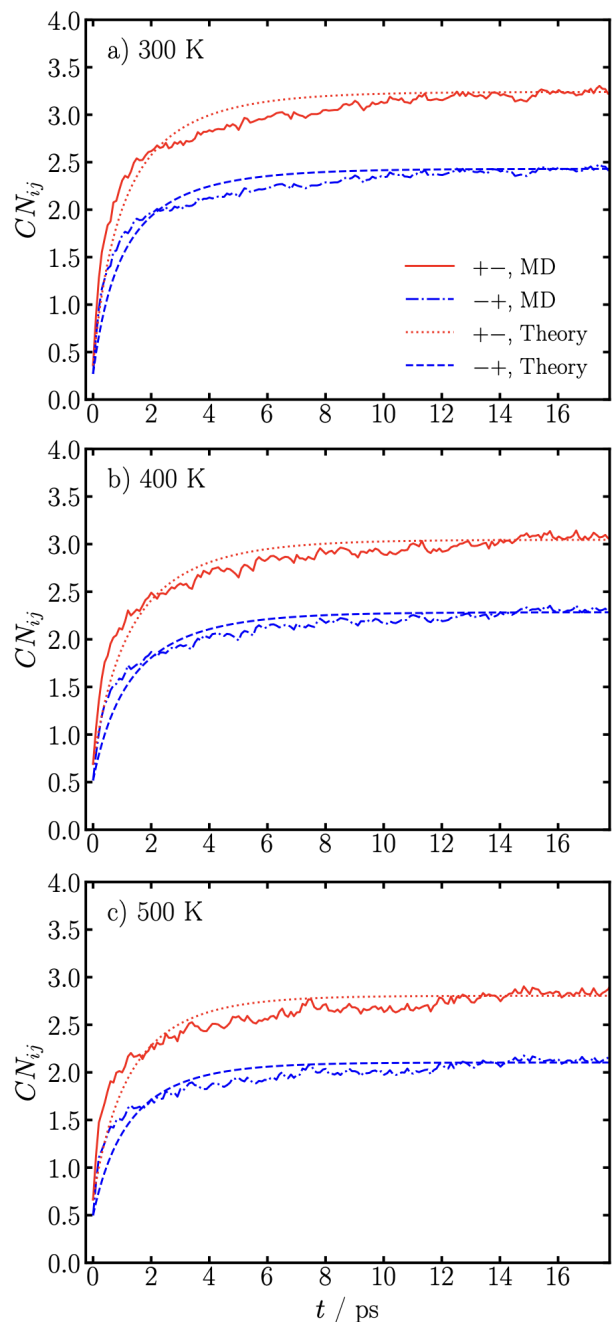


FIG. 2. Coordination numbers between  $\text{Na}^+$  and  $\text{TFSI}^-$  in  $\text{NaTFSI}_{0.75}\text{EMIMTFSI}_{0.25}$  as a function of time, for the charge rescaling case, at the indicated temperatures, from MD simulations and theory.

each curve ( $CN_{+-}$  and  $CN_{-+}$ ) gives essentially (within several decimal places) the same inverse decay time of  $\sim 0.4 \text{ ps}^{-1}$ . This corresponds to a decay time of  $\sim 2.5 \text{ ps}$ , which agrees well with the time scale observed in Fig. 2a). Using this fitted decay constant, we plot the theory prediction in Fig. 2a), where reasonable agreement is found. Moreover, using Eq. (26), we can use this information to extract the rate constant of forming associations,  $k$ ,

$T / \text{K}$	$\tau^{-1} / \text{ps}^{-1}$	$k / \text{ps}^{-1}$	$\lambda$
300	0.401	3.000	71.178
400	0.418	2.398	42.383
500	0.511	2.231	24.880

TABLE I. Summary of inverse time scales ( $\tau^{-1}$ ), rate of forming an association ( $k$ ), and association constant for the studied temperatures of the symmetric case.

which we also report in Tab. I. We find a value of  $3 \text{ ps}^{-1}$  for the rate of forming associations, which is larger than the fitted inverse time constant and can be attributed to the rate of forming associations needing to be faster than the observed inverse rate constant, since they are reversible associations.

In Fig. 2b)&c), we show analogous non-equilibrium coordination numbers as a function of time for 400 k and 500 k, respectively. Again fitting these (using the initial and final association probabilities from MD) provides the time constants  $\sim 0.41$  and  $\sim 0.51 \text{ ps}^{-1}$ , for 400 K and 500 K, respectively; and we find that the fitted decay constant for the theory results in a reasonable fit to the MD simulations for 400 K and 500 K. With increasing temperature, we observe the inverse time constant to increase, indicating the time constant decreases with temperature. Intuitively, this makes sense, since at higher temperatures the associations will be weaker, which should therefore take less time to form. In Tab. I, we also report the association constant at the studied temperatures, where we find it decreases with temperature. Again, using Eq. (26) we can extract the rate constant of forming an association,  $k$ , and find  $\sim 2.4$  and  $\sim 2.2 \text{ ps}^{-1}$ , for 400 K and 500 K, respectively. These are summarized in Tab. I. With increasing temperature, we find  $k$  decreases. If the process was to be activated,  $\propto e^{-\beta E_a}$ , it should increase with temperature. This suggests that the activation barrier, if present, is not large, and other factors are dominating the rate of forming an association.

While the theory also has an initial rapid increase over  $\sim 2 \text{ ps}$ , and slower increase after, the quantitative agreement with the MD simulations is not exact (same conclusion is obtained from the temperature rescaling simulations, see SI). We find that the theory under-predicts the MD simulation results at short times, but over-predicts the values of the coordination numbers at long times. The only variable that could cause this disagreement is the decay constant, or more specifically the rate constants of forming and breaking an association. Since a single value of this rate of forming an association does not well fit the data, it suggests that there is more than one time scale in the simulations.

To investigate this further, we calculated the decay of the associations over time of, which can be used to extract residence/persistence times (see Molecular Dynamics Methods for the calculation). In other words, at an initial time in an equilibrium simulation, we counted the number of associations that remained after some given

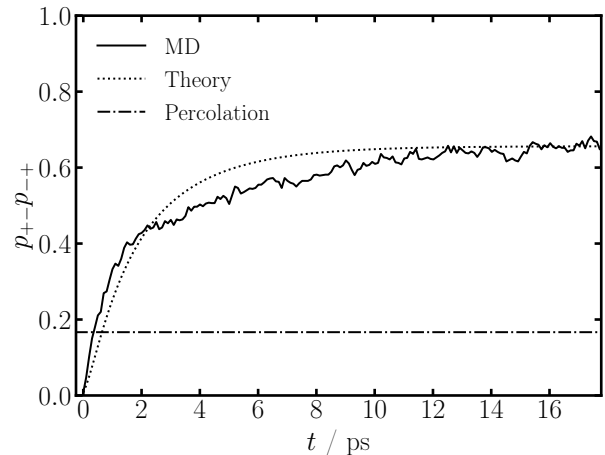


FIG. 3. Gelation criteria in  $\text{NaTFSI}_{0.75}\text{EMIMTFSI}_{0.25}$  as a function of time, for the charge rescaling case, at 300 K, for MD and theory. The percolation point is given by  $p_+ - p_{-+} = [(f_+ - 1)(f_- - 1)]^{-1}$ .

time. Therefore, we start from 100% of the associations at the initial time, which decays if the associations between those cations and anions break. This is similar to the irreversible fragmentation solution discussed in the symmetric case. However, from the simulations, if those exact associations between a specific cation and anion reform, this can also cause this measure to momentarily increase, which would not be possible in the irreversible aggregation case. However, since species tend to diffuse and associate with other ions after dissociating, this measure generally decays with time, and should approximately follow a single exponential decay if there is one rate constant (as found for the irreversible fragmentation). In the SI, we show this result for  $\text{NaTFSI}_{0.75}\text{EMIMTFSI}_{0.25}$  at 300 K. What we find is that initially the initial associations decay by 10-20% very rapidly over several picoseconds. After which, the decay of the initial associations becomes more gradual, and only changes over a  $\sim \text{ns}$  time scale. Similar results were found by Molinari *et al.* for similar SiILs [13], Self and Fong in the context of battery electrolytes [92, 93], and by Feng *et al.* in the context of ILs [97]. Therefore, there are clearly multiple time-scales for the kinetics of aggregate formation in SiILs.

To test this further, we fitted the coordination numbers over time, but only for first 5 ps. In the SI we show these fits, where much better agreement is found, since it is described by a single, fast association-forming time scale ( $\tau^{-1} \approx 1 \text{ ps}^{-1}$ ). Moreover, we also show that the coordination numbers increase slightly from the values in Fig. 2 over 10s of ps time scales. Therefore, in the MD simulations, the coordination numbers are initially controlled by the fast rate constant of forming associations of species that are already in proximity to each other, but at longer time scales this rate constant becomes limited by the diffusion/rearrangement of the electrolyte (not associations, since they should already be

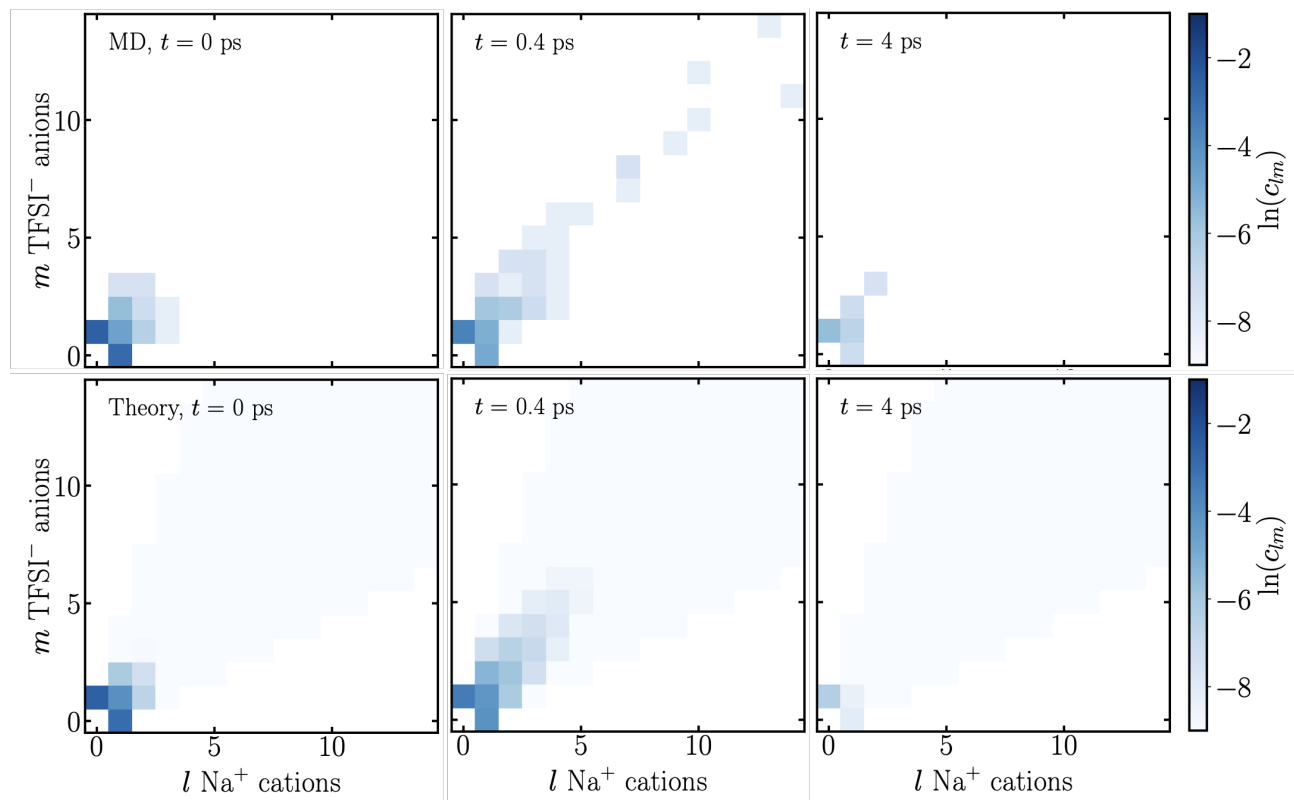


FIG. 4. Cluster distributions  $c_{lm}$ , with  $m$  TFSI<sup>-</sup> anions and  $l$  Na<sup>+</sup> cations in an aggregate, at various times in the MD simulation and theory, as indicated, at 300 K.

accounted for) to allow for the equilibrium associations to be reached [92, 93]. This explains why the theory underestimating the MD are short time scales, but overestimating the MD at long time scales. These observations pose a fundamental limitation of the theory, which assumes one rate constant, and motivates its development further. While the theory is not a perfect quantitative fit, it still provides insight into the underlying dynamics, and we further investigate it.

Using the time evolving association probabilities, we can determine at what time a percolating ionic network, i.e., a gel, between Na<sup>+</sup> and TFSI<sup>-</sup> should form. This can be achieved through tracking the product of the association probabilities,  $p_{+-}p_{-+}$ . When this value reaches  $[(f_+ - 1)(f_- - 1)]^{-1}$ , that is the critical criteria for bond percolation on a Bethe lattice, i.e., a Cayley tree [53, 57]. In SiILs, the percolating ionic network is known to occur at  $x \approx 0.25$  from simulations [56]; while the theory predicts it at smaller mole fractions, owing to the formation of loops in the clusters [15, 56].

In Fig. 3 we show  $p_{+-}p_{-+}$  as a function of time for NaTFSI<sub>0.75</sub>EMIMTFSI<sub>0.25</sub> at 300 K. From the MD simulations, we find that the critical criteria for form a gel is already satisfied after  $\sim 0.5$  ps. The theory predicts the percolating ionic network to form at  $\sim 1$  ps, but this is because the theory is underestimating the association probabilities at short times.

To check if the critical gel criteria is actually being satisfied in the simulations, we can inspect the cluster distribution [53, 56, 57]. If we are in a pre-gel regime, we only expect small clusters (relative to the simulation size) to occur. As we approach the gel-point, the concentration of larger clusters continuously grows. When the gel-point is reached, there is simultaneously aggregates of all sizes and an aggregate that percolates throughout the simulation cell. In the post-gel regime, larger aggregates bind to the gel, increasing the gels volume fraction, leaving only small clusters. See Refs. 53, 56, 57 for more information.

In Fig. 4, we show the cluster distribution computed from MD simulations and theory at 3 times. At  $t = 0$ , we find that free anions and cations dominate, with a smaller number of ion pairs, and even fewer aggregates containing a handful of ions. At  $t = 0.4$  ps, right at the critical gel time, we find that free anions still dominate the cluster distribution (as they usually do for SiILs [15, 56]), but there are aggregates which exist with over 30 ions. At this time, we also find a single aggregate with a significant portion of the ions in the simulation cell. At later times than  $t = 0.4$  ps, the size of the aggregates decreases steadily. We show an example at  $t = 4$  ps, where free anions still dominate, and there are at most 5 ions in an aggregate, which is smaller than when the charges were scaled to practically 0 at  $t = 0$  ps. There-

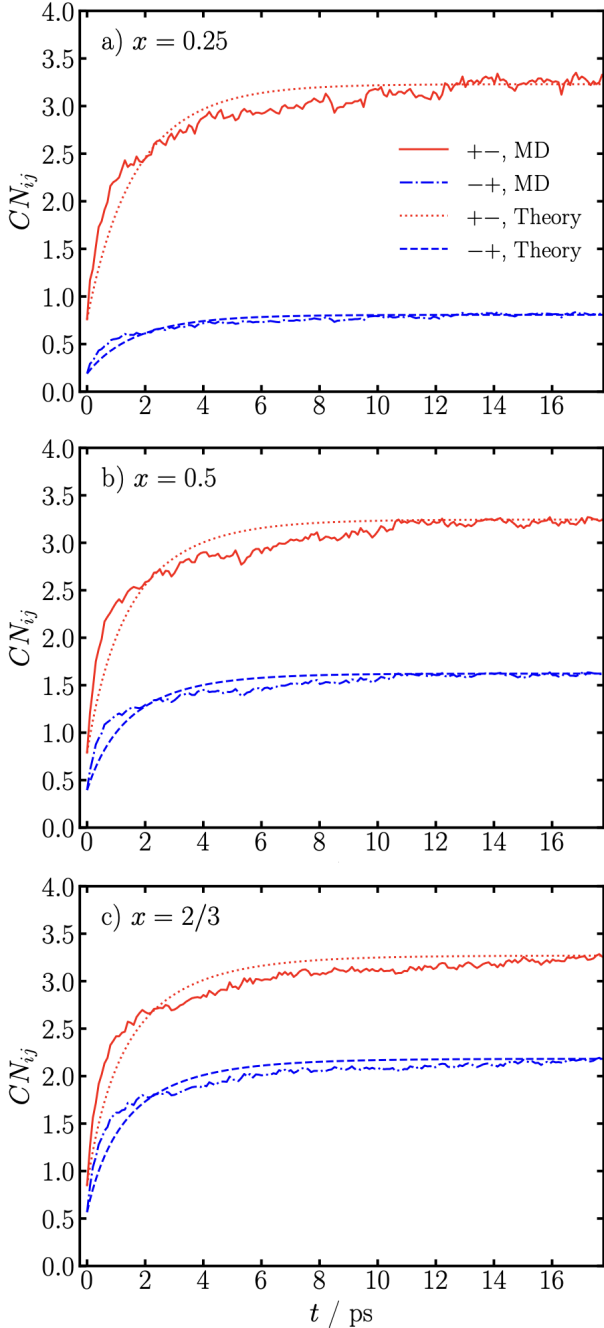


FIG. 5. Coordination numbers between  $\text{Na}^+$  and  $\text{TFSI}^-$  as a function of time, for the charge rescaling case, for the indicated mole fractions, in  $\text{NaTFSI}_x\text{EMIMTFSI}_{1-x}$ , at 300 K, for MD simulations and theory.

fore, the critical gel-time of the simulation predicted in Fig. 3 corresponds well to the behavior of the aggregates in the simulation, shown in Fig. 4, confirming the bond percolation criteria [53, 56, 57]. The theory predictions (calculated with the cluster distribution, and the association probabilities and association constant changing in time) match the simulated ones qualitatively very well.

Previously, for SiILs, as discussed in Ref. 56, the theory cluster distribution did not agree well with that of the MD simulations, owing to the presence of loops in the aggregates [15]. In the SI, we computed the cluster bond density, which quantifies how many loops exist in the aggregates. Unlike the equilibrium case [15], we only find a few loops, which could be why good agreement is obtained here.

## B. Asymmetric case

In this section we further test the asymmetric case of the equations. Analogous observations are found to the symmetric case, but it further cements those findings.

In Fig. 5 we show how  $CN_{ij}$  changes with time, again from the charge rescaling non-equilibrium simulations, for the indicated mole fractions  $x$  in  $\text{NaTFSI}_x\text{EMIMTFSI}_{1-x}$  at 300 K. For the lowest mole fraction case,  $x = 0.25$ , as seen in Fig. 5a), using the initial and final probabilities from MD, we fitted a decay time of  $\sim 0.52 \text{ ps}^{-1}$ , and a rate constant of forming an association of  $\sim 2.2 \text{ ps}^{-1}$ . Overall, the theory again does a reasonable job at capturing the trends in the simulations, although it again underestimates the coordination numbers at short times and overestimate them at long times. Very similar observations are found for the mole fractions of  $x = 0.5$  and  $x = 2/3$ , as shown in Fig. 5b)&c), respectively.

In Tab. II, we report the fitted parameters of our model. With increasing mole fraction of Na-salt, the association constant increases substantially, which is consistent with the expectation of IL cations interacting with the  $\text{TFSI}^-$  anions [56]. We find the inverse time scale  $\tau^{-1}$  decreases with increasing mole fraction of Na-salt, which indicates the time scale increases with increasing mole fraction of Na-salt. Since the associations are becoming stronger, this intuitively makes sense. We find the rate of forming associations increases with increasing mole fraction of Na-salt, suggesting it is becoming easier to form associations in more Na-rich environments.

For the  $x = 0.25$  and  $x = 0.5$  mole fractions, we predict the critical times of gelation in Fig. 6. For the  $x = 0.25$  case, as shown in Fig. 6a), the electrolyte at long times only just resides above the critical condition to form a percolating ionic network. We find that at  $\sim 4 \text{ ps}$ , both MD simulations and theory predict the transition into the gel regime. Whereas, for the  $x = 0.5$  case, as shown in Fig. 6b), the electrolyte is well in the gel regime. The MD simulations predict a critical gel time at  $\sim 0.75 \text{ ps}$ , while the theory lags behind these simulations at  $\sim 1 \text{ ps}$ .

In Fig. 7, we plot the calculated cluster distributions from MD simulations and theory at various times for the mole fractions  $x = 0.25$  and  $x = 0.5$ . In the top rows, which corresponds to  $x = 0.25$ , free ions initially ( $t = 0$ ) dominate the simulations, with a small concentration of aggregates containing fewer than 5 ions. At  $t = 6 \text{ ps}$ , which should correspond to the electrolyte having en-

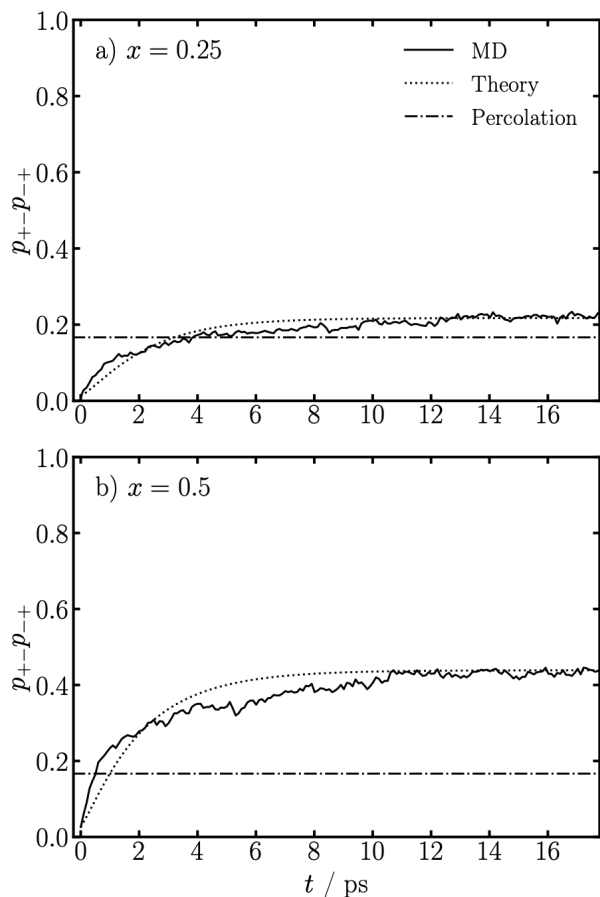


FIG. 6. Gelation criteria as a function of time for different alkali metal mole fractions in  $\text{NaTFSI}_x\text{EMIMTFSI}_{1-x}$ , for the charge rescaling case, at 300 K, for MD simulations and theory. The percolation point is given by  $p_{+-}p_{-+} = [(f_+ - 1)(f_- - 1)]^{-1}$ .

$x$	$\tau^{-1} / \text{ps}^{-1}$	$k / \text{ps}^{-1}$	$\lambda$
1/4	0.517	2.223	23.916
1/2	0.478	2.535	34.322
2/3	0.403	3.214	54.736

TABLE II. Summary of inverse time scales ( $\tau^{-1}$ ), rate of forming an association ( $k$ ), and association constant for the studied compositions of the asymmetric case.

tered the gel regime, we find aggregates containing up to 20 ions, but with free anions still dominating the distribution and no free cations existing. In addition, we find a percolating ionic network in the simulation. At a later time,  $t = 15$  ps, we find practically the same cluster distribution. In Fig. 6,  $p_{+-}p_{-+}$  does not grow substantially over the critical point, so the changes in the cluster distribution follow well these predictions form the critical gel criteria.

Whereas, for  $x = 0.5$ , as shown the bottom row of Fig. 7, we find results more similar to the symmetric case previously described. At  $t = 0.8$  ps, which is a time

just larger the predicted critical gel time in Fig. 6b), we find a large distribution of aggregates, containing up to 30 ions, in addition to a percolating ionic network. At a later time of  $t = 4$  ps, the cluster distribution is again diminished, with practically only free anions and no free cations.

Therefore, the cluster distributions further corroborate the predicted critical gel times from the association probabilities. Furthermore, this also supports the idea that the central variable is the association probabilities, which changes in time, and is used in the cluster distribution in a quasi-equilibrium way, with the theory predictions qualitatively matching the simulated values.

## V. DISCUSSION

To summarize, we developed the kinetics of aggregation formalism of Sciortino, Tartaglia and co-workers [75–77, 80–84] from patchy particle systems to work for concentrated electrolyte systems, extending the equilibrium and linear-response formalism developed by McEldrew *et al.* [23, 53, 55–58]. Comparisons to molecular dynamics simulations found good qualitative agreement, but quantitative differences were found. These were investigated further, and found to result from multiple time scales existing in the concentrated electrolyte [13, 92, 93]. Specifically, there is a fast time at short times, corresponding to associations forming between species that are in close proximity. After which the time scale slows, being more limited by diffusion and rearrangements of ions [92]. While the theory is not quantitative, it does provide insight into the overall mechanisms occurring and a framework to understand them. For example, we also demonstrated that the quasi-equilibrium solution applies to SiILs, where the cluster distribution changes in time from the changes in association probabilities, with this quasi-equilibrium solution connecting time and temperature through the association probabilities, since it can be thought that  $p(t)$  is changing through equilibrium states of  $p(T)$  [75–77, 80–84].

Interestingly, using this formalism, we extracted the rate for the formation of an association, which was found to vary slightly with temperature and composition of the electrolyte. In the context of the temperature dependence, an exponential law might be expected for an activated process, and moreover, for the rate to increase with increasing temperature. Since we do not observe this, it suggests this process is not an activated one. While in the context of different compositions, changes in dielectric environment and viscosity might also be expected to change these rates substantially. However, we also do not observe strong effects from these variables. It is known that residence times of different SiILs [13], ILs [97], WiSEs [57] and battery electrolytes [92] can vary, which suggests different rates of forming associations. Future work should investigate these observations in more depth, for different electrolytes, different tem-

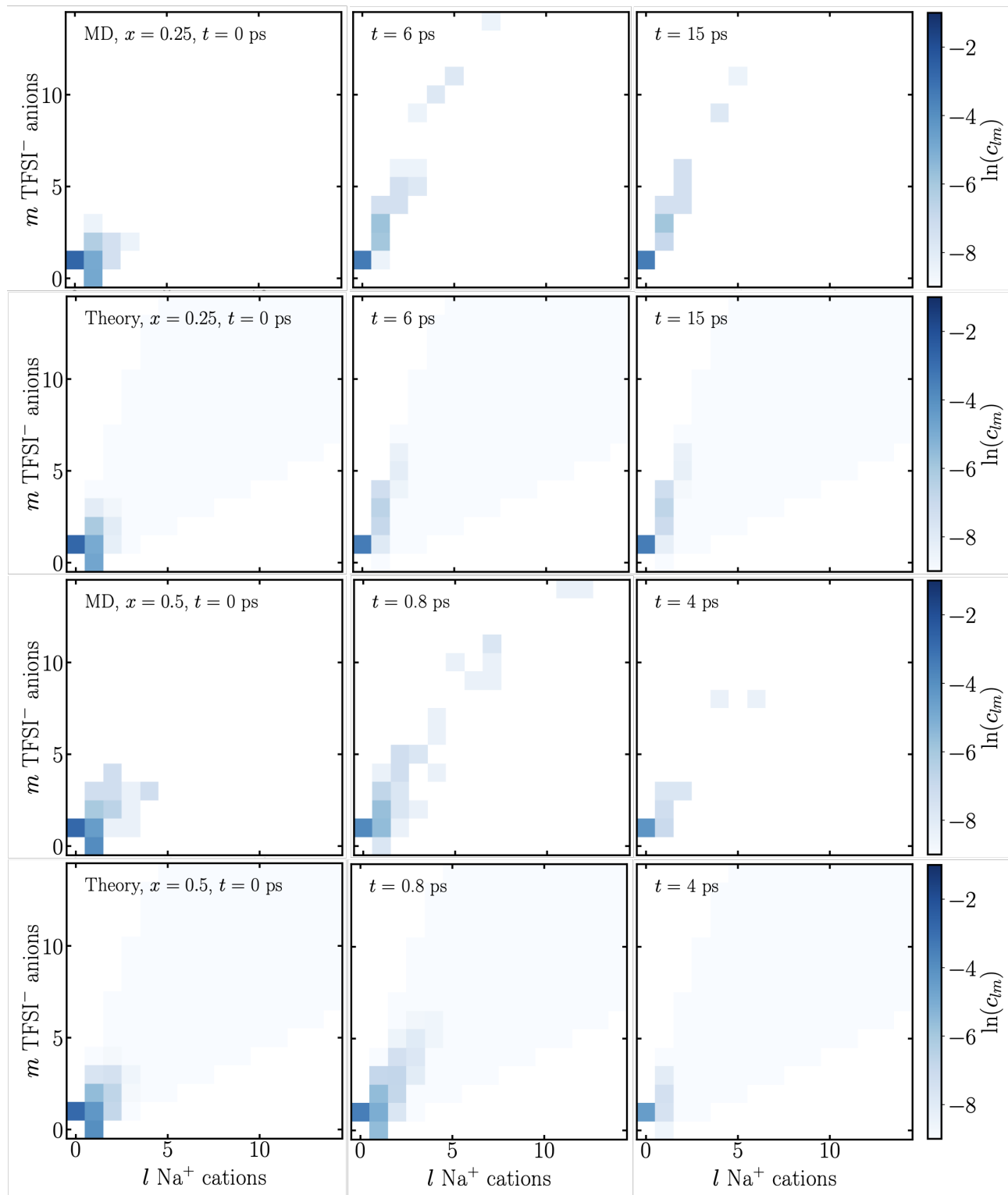


FIG. 7. Cluster distributions  $c_{lm}$ , with  $m$  TFSI<sup>-</sup> anions and  $l$  Na<sup>+</sup> cations in an aggregate, at various points in the MD simulations and theory, as indicated, at 300 K for the different alkali metal mole fractions in NaTFSI<sub>x</sub>EMIMTFSI<sub>1-x</sub>.

peratures, and investigate the role of multiple time scales more thoroughly.

It is hoped that this provides the first link between a microscopic theory of ionic associations and non-equilibrium changes to electrolyte structure, which is further built upon. In what follows, we outline possible extensions and connections to other areas in concentrated electrolytes. While this is not an exhaustive list, we hope it provides inspiration for what might now be possible.

In the context of ionic transport in concentrated electrolytes, there is simultaneously vehicular motion of the aggregates/clusters and structural diffusion [92, 93]. To determine the dominant mechanism Self and Fong *et al.* [92, 93] suggested comparing length scales of the aggregates ( $L^s$ ) to the length scales over which they move in a vehicular was. The later is determined from  $L^c = \sqrt{6D_i\tau_{res}}$ , where  $D_i$  is the self diffusion coefficient and  $\tau_{res}$  is the residence time of the association. If  $L^c > L^s$ , there is vehicular dominated motion, while if  $L^c < L^s$  it is structural dominated motion. There are clearly multiple time scales for associations in electrolytes, as found here for SiILs, and by others [13, 57, 92, 93, 97]. Self and Fong *et al.* [92, 93] suggested using the long-time scale, and ignoring the short, sub-diffusive changes in associations. If the short time scale is used, which is attributed to the binding/breaking of associations in proximity, this would suggest structural diffusion dominates more. While if the long time scale is used, it suggest more of a vehicular motion could be dominant. The results here suggest that this short-time scale is important, indicating that transport in these electrolytes could be more dominated by structural diffusion. Using the formalism developed here, it might be possible to more quantitatively link vehicular and structural diffusion modes.

As discussed in the Results and Theory Sections, concentrated electrolytes have been predicted to form a percolating ionic network, i.e., a gel phase [53, 55–57] (to date, only one experimental claim of a gel from associations has been reported [98]). The terminology of the gel phase comes from the inherited language from polymer systems [63–74]. In thermoreversible polymers the time scales of the associations are much longer than electrolytes, since the associations are much stronger. Upon gelation, this gives rise to a divergence in viscosity and the onset of an elastic response [53]. It is not clear if the elastic response will be measurable from the shorter time scales of the associations in concentrated electrolytes, however. In the context of experimental measurements, non-Newtonian behavior of WiSEs has been measured [47], suggesting that in WiSE these associations could be long-lived enough. Significantly more work is required in this area, from theory, simulations and experiments, to understand how similar electrolytes are to polymers in this regard, i.e., how good the analogy between ionic associations and thermoreversible bonds. Using the developed formalism, it should be possible to include the finite time scales of associations, to more quantitatively predict the frequency dependence of the

viscous and elastic response of the fluid [85, 86].

Here we have only studied bulk electrolytes, but the technologies which use these electrolytes often require contact with electrified interfaces [9, 20, 21, 99]. How concentrated electrolytes accumulate at electrified interfaces, i.e., the electrical double layers (EDL), has been studied at equilibrium in the context of McEldrew *et al.*'s formalism for ILs [59, 60], SiILs [15, 62] and WiSEs [61]. Using the formalism developed here, the charging dynamics of the EDL could be studied with the relaxation of the aggregates. While the aggregation relaxation time scale appears to be faster than the electrolyte transport, studying the relaxation of aggregates in confinement could result in interesting interplay with the transport of ions. Building on this, the desolvation dynamics of battery electrolytes at the electrodes would be another area to investigate, to more quantitatively determine the time scales involving how the solvation shell is stripped from the active cation as it intercalates into the electrode. As a first step, the removal of one solvent from the diffuse EDL to Helmholtz layer could be investigated [100], building all the way up to the complete removal and intercalation of the active ion.

Finally, in the context of “anomalous underscreening” [33–39, 101], it has been shown that with slower approaches of the interfaces the long-ranged interactions vanish [40]. Therefore, this effect is not from bulk electrostatic interactions, but a large part is the hydrodynamic interactions [15, 40]. It remains to be seen if it can be completely described by classical fluid mechanics, however. In confinement with these concentrated electrolytes, the ionic aggregation effects could also be playing a role [15]. In the context of SiILs, Zhang *et al.* [15] found force separation, extremely long force decay lengths, and changes in refractive indices of the electrolyte between mica. This made them conclude there was confinement induced changes in electrolyte composition, possibly leading to the formation of a gel [15]. Further developing the formalism here to confined geometries, also with changing composition, could provide insight into the role of ionic aggregation kinetic in these measurements. We have found that the time scale of ionic aggregation  $\tau$  can diverge if the association probabilities approach 1, which could give rise to extremely long relaxation times. However, the short-time scale of association appears to be of the order of  $\sim$ ps (which could also arise from the finite size of the simulation cells). Further work should explore if the aggregate relaxations could help explain these puzzling non-equilibrium measurements.

## VI. ACKNOWLEDGMENTS

I am extremely grateful for the support and stimulating discussion from M. McEldrew, A. Kornyshev, C. Phelan and R. Espinosa-Marzal. I also acknowledge discussions with P. de Souza, R. Weatherup, N. Molinari, M. Markiewitz and M. Bazant. Z.A.H.G acknowledges

support through the Glasstone Research Fellowship in

Materials and The Queen’s College, University of Oxford.

- 
- [1] L. Suo, Y.-S. Hu, H. Li, M. Armand, and L. Chen, *Nat. Commun.* **4**, 1481 (2013).
- [2] L. Suo, O. Borodin, T. Gao, M. Olguin, J. Ho, X. Fan, C. Luo, C. Wang, and K. Xu, *Science* **350**, 938 (2015).
- [3] J. Wang, Y. Yamada, K. Sodeyama, C. H. Chiang, Y. Tateyama, and A. Yamada, *Nat. Commun.* **7**, 12032 (2016).
- [4] F. Wang, O. Borodin, T. Gao, X. Fan, W. Sun, F. Han, A. Faraone, J. A. Dura, K. Xu, and C. Wang, *Nature Materials* **17**, 543 (2018).
- [5] Y. Yamada, K. Usui, K. Sodeyama, S. Ko, Y. Tateyama, and A. Yamada, *Nat. Energy* **1**, 16129 (2016).
- [6] L. Suo, O. Borodin, Y. Wang, X. Rong, W. Sun, X. Fan, S. Xu, M. A. Schroeder, A. V. Cresce, F. Wang, *et al.*, *Advanced Energy Materials* **7**, 1701189 (2017).
- [7] Q. Dou, S. Lei, D.-W. Wang, Q. Zhang, D. Xiao, H. Guo, A. Wang, H. Yang, Y. Li, S. Shi, and X. Yan, *Energy Environ. Sci.* **11**, 3212 (2018).
- [8] A. A. Kornyshev, *J. Phys. Chem. B* **111**, 5545 (2007).
- [9] M. V. Fedorov and A. A. Kornyshev, *Chem. Rev.* **114**, 2978 (2014).
- [10] T. Welton, *Chem. Rev.* **99**, 2071–2084 (1999).
- [11] J. P. Hallett and T. Welton, *Chem. Rev.* **111**, 3508–3576 (2011).
- [12] N. Molinari, J. P. Mailoa, and B. Kozinsky, *J. Phys. Chem. Lett.* **10**, 2313 (2019).
- [13] N. Molinari, J. P. Mailoa, N. Craig, J. Christensen, and B. Kozinsky, *J. Power Sources* **428**, 27 (2019).
- [14] N. Molinari and B. Kozinsky, *J. Phys. Chem. B* **124**, 2676 (2020).
- [15] X. Zhang, Z. A. Goodwin, A. G. Hoane, A. Dep-tula, D. M. Markiewitz, N. Molinari, Q. Zheng, H. Li, M. McEldrew, B. Kozinsky, *et al.*, *ACS nano* **18**, 34007 (2024).
- [16] K. Xu, *Chem. Rev.* **104**, 4303 (2004).
- [17] J. B. Goodenough and K. S. Park, “The Li-ion rechargeable battery: A perspective,” (2013).
- [18] K. Xu, *Chem. Rev.* **114**, 11503 (2014).
- [19] M. Li, C. Wang, Z. Chen, K. Xu, and J. Lu, *Chem. Rev.* (2020).
- [20] M. A. Gebbie, B. Liu, W. Guo, S. R. Anderson, and S. G. Johnstone, *ACS Catal.* **13**, 16222 (2023).
- [21] J. Zheng, J. A. Lochala, A. Kwok, Z. D. Deng, and J. Xiao, *Adv. Sci.* **4**, 1700032 (2017).
- [22] C. M. Phelan, E. Björklund, J. Singh, M. Fraser, P. N. Didwal, G. J. Rees, Z. Ruff, P. Ferrer, D. C. Grin-ter, C. P. Grey, *et al.*, *Chemistry of Materials* **36**, 3334 (2024).
- [23] C. Phelan, A. Bhandari, J. Singh, M. F. nad Erik Björklund, J. Swallow, P. Bencok, C. Grey, Z. Goodwin, C. Skylaris, and R. Weatherup, <https://chemrxiv.org/doi/pdf/10.26434/chemrxiv-2025-k903g> (2025).
- [24] Z. Yu, L. A. Curtiss, R. E. Winans, Y. Zhang, T. Li, and L. Cheng, *The Journal of Physical Chemistry Letters* **11**, 1276 (2020).
- [25] O. Borodin, L. Suo, M. Gobet, X. Ren, F. Wang, A. Faraone, J. Peng, M. Olguin, M. Schroeder, M. S. Ding, *et al.*, *ACS nano* **11**, 10462 (2017).
- [26] P. Lannelongue, R. Bouchal, E. Mourad, C. Bodin, M. Olarte, S. le Vot, F. Favier, and O. Fontaine, *Journal of The Electrochemical Society* **165**, A657 (2018).
- [27] J. Vatamanu and O. Borodin, *J. Phys. Chem. Lett.* **8**, 4362 (2017).
- [28] L. G. Chagas, S. Jeong, I. Hasa, and S. Passerini, *ACS Appl. Mater. Interfaces* **11**, 22278 (2019).
- [29] T. C. Lourenco, L. G. Dias, and J. L. Da Silva, *ACS Appl. Energy Mater.* **4**, 4444 (2021).
- [30] R.-S. Kühnel, D. Reber, and C. Battaglia, *ACS Energy Lett.* **2**, 2005 (2017).
- [31] O. Borodin, J. Self, K. A. Persson, C. Wang, and K. Xu, *Joule* **4**, 69 (2020).
- [32] Z. Yu, N. P. Balsara, O. Borodin, A. A. Gewirth, N. T. Hahn, E. J. Maginn, K. A. Persson, V. Srinivasan, M. F. Toney, K. Xu, K. R. Zavadil, L. A. Curtiss, and L. Cheng, *ACS Energy Lett.* **7**, 461 (2022).
- [33] M. A. Gebbie, M. Valtiner, X. Banquy, E. T. Fox, W. A. Henderson, and J. N. Israelachvili, *Proceedings of the National Academy of Sciences* **110**, 9674 (2013).
- [34] M. A. Gebbie, H. A. Dobes, M. Valtiner, and J. N. Israelachvili, *Proceedings of the National Academy of Sciences* **112**, 7432–7437 (2015).
- [35] M. Han, H. Kim, C. Leal, M. Negrito, J. D. Batteas, and R. M. Espinosa-Marzal, *Adv Mater Interfaces* **7**, 2001313 (2020).
- [36] M. Han, R. Zhang, A. A. Gewirth, and R. M. Espinosa-Marzal, *Nano Lett.* **21**, 2304 (2021).
- [37] T. S. Groves, C. S. Perez-Martinez, R. Lhermerout, and S. Perkin, *The Journal of Physical Chemistry Letters* **12**, 1702 (2021).
- [38] A. M. Smith, A. A. Lee, and S. Perkin, *J. Phys. Chem. Lett.* **7**, 2157 (2016).
- [39] C. S. Perez-Martinez, A. M. Smith, S. Perkin, *et al.*, *Faraday discussions* **199**, 239 (2017).
- [40] B. Cross, L. Garcia, E. Charlaix, and P. Kekicheff, *PNAS* **123**, e2517939123 (2026).
- [41] A. Härtel, M. Bültmann, and F. Coupette, *Physical Review Letters* **130**, 108202 (2023).
- [42] R. Kjellander, *Physical Chemistry Chemical Physics* **18**, 18985 (2016).
- [43] Y. Avni, R. M. Adar, and D. Andelman, *Physical Review E* **101**, 010601 (2020).
- [44] R. M. Adar, S. A. Safran, H. Diamant, and D. Andelman, *Physical Review E* **100**, 042615 (2019).
- [45] J. P. de Souza, Z. A. Goodwin, M. McEldrew, A. A. Kornyshev, and M. Z. Bazant, *Phys. Rev. Lett.* **125**, 116001 (2020).
- [46] E. Krucker-Velasquez and J. W. Swan, *The Journal of Chemical Physics* **155**, 134903 (2021).
- [47] T. Yamaguchi, A. Dukhin, Y.-J. Ryu, D. Zhang, O. Borodin, M. A. González, O. Yamamuro, D. L. Price, and M.-L. Saboungi, *J. Phys. Chem. Lett.* **15**, 76 (2024).

- [48] Y. S. Meng, V. Srinivasan, and K. Xu, *Science* **378**, 1065 (2022).
- [49] O. Borodin and D. Bedrov, *J. Phys. Chem. C* **118**, 18362 (2014).
- [50] O. Borodin, X. Ren, J. Vatamanu, A. von Wald Cresce, J. Knap, and K. Xu, *Acc. Chem. Res.* **50**, 2886 (2017).
- [51] Q. Wu, M. T. McDowell, and Y. Qi, *JACS* **145**, 2473 (2023).
- [52] A. V. Tkachenko, C. Cao, A. C. Marschilok, and D. Lu, arXiv:2512.18167 (2025).
- [53] M. McEldrew, Z. A. Goodwin, S. Bi, M. Z. Bazant, and A. A. Kornyshev, *J. Chem. Phys.* **152**, 234506 (2020).
- [54] M. McEldrew, *Ion Aggregation, Correlated Ion Transport and the Double Layer in Super-Concentrated Electrolytes*, Ph.D. thesis, MIT (2021).
- [55] M. McEldrew, Z. A. H. Goodwin, H. Zhao, M. Z. Bazant, and A. A. Kornyshev, *J. Phys. Chem B* **125**, 2677–2689 (2021).
- [56] M. McEldrew, Z. A. H. Goodwin, N. Molinari, B. Kozinsky, A. A. Kornyshev, and M. Z. Bazant, *J. Phys. Chem. B* **125**, 13752 (2021).
- [57] M. McEldrew, Z. A. Goodwin, S. Bi, A. Kornyshev, and M. Z. Bazant, *J. Electrochem. Soc.* **168**, 050514 (2021).
- [58] Z. A. H. Goodwin, M. McEldrew, B. Kozinsky, and M. Z. Bazant, *PRX Energy* **2**, 013007 (2023).
- [59] Z. A. Goodwin, M. McEldrew, J. P. de Souza, M. Z. Bazant, and A. A. Kornyshev, *J. Chem. Phys.* **157**, 094106 (2022).
- [60] Z. A. Goodwin and A. A. Kornyshev, *Electrochim. Acta* **434**, 141163 (2022).
- [61] D. M. Markiewitz, Z. A. Goodwin, Q. Zheng, M. McEldrew, R. M. Espinosa-Marzal, and M. Z. Bazant, *ACS Applied Materials & Interfaces* **17**, 29515 (2025).
- [62] D. M. Markiewitz, Z. A. Goodwin, M. McEldrew, J. P. de Souza, X. Zhang, R. M. Espinosa-Marzal, and M. Z. Bazant, *Faraday Discussions*, 365 (2024).
- [63] P. J. Flory, *The Journal of chemical physics* **10**, 51 (1942).
- [64] W. H. Stockmayer, *The Journal of chemical physics* **11**, 45 (1943).
- [65] W. H. Stockmayer, *The Journal of Chemical Physics* **12**, 125 (1944).
- [66] W. H. Stockmayer, *J. Polym. Sci.* **9**, 69 (1952).
- [67] M. Ishida and F. Tanaka, *Macromolecules* **30**, 3900 (1997).
- [68] F. Tanaka, *Macromolecules* **22**, 1988 (1989).
- [69] F. Tanaka, *Macromolecules* **23**, 3784 (1990).
- [70] F. Tanaka and W. H. Stockmayer, *Macromolecules* **27**, 3943 (1994).
- [71] F. Tanaka and M. Ishida, *J. Chem. Soc. Faraday Trans.* **91**, 2663 (1995).
- [72] F. Tanaka, *Physica A: Statistical Mechanics and its Applications* **257**, 245 (1998).
- [73] F. Tanaka and M. Ishida, *Macromolecules* **32**, 1271 (1999).
- [74] F. Tanaka, *Polym. J.* **34**, 479 (2002).
- [75] F. Sciortino and E. Zaccarelli, *Current Opinion in Solid State and Materials Science* **15**, 246 (2011).
- [76] F. Sciortino, C. D. Michele, S. Corezzi, J. Russo, E. Zaccarelli, and P. Tartaglia, *Soft Matter* **5**, 2571 (2009).
- [77] S. Corezzi, D. Fioretto, and F. Sciortino, *Soft Matter* **8**, 11207 (2012).
- [78] A. Gröschel, A. Walther, T. I. Löbbling, F. H. Schacher, H. Schmalz, and A. H. E. Müller, *Nature* **503**, 247 (2013).
- [79] A. Umar and S.-M. Choi, *J. Phys. Chem. C* **117**, 11738 (2013).
- [80] S. Corezzi, D. Fioretto, C. D. Michele, E. Zaccarelli, and F. Sciortino, *J. Phys. Chem. B* **114**, 3769 (2010).
- [81] E. Bianchi, P. Tartaglia, E. L. Nave, and F. Sciortino, *J. Phys. Chem. B* **111**, 11765 (2007).
- [82] S. Corezzi, C. D. Michele, E. Zaccarelli, P. Tartaglia, and F. Sciortino, *J. Phys. Chem. B* **113**, 1233 (2009).
- [83] F. Sciortino, C. D. Michele, and J. F. Douglas, *J. Phys.: Condens. Matter* **20**, 155101 (2008).
- [84] P. Tartaglia, *J. Phys.: Condens. Matter* **21**, 504109 (2009).
- [85] F. Tanaka, *Macromolecules* **57**, 10600 (2024).
- [86] F. Tanaka, *Gels* **9**, 379 (2023).
- [87] K. Xu and A. von Wald Cresce, *J. Mater. Res.*, Vol. , No. 18, Sep 28, **27**, 2327 (2012).
- [88] Z. Tian, Y. Zou, G. Liu, Y. Wang, J. Yin, J. Ming, and H. N. Alshareef, *Adv. Sci.* **9**, 2201207 (2022).
- [89] T. Welton, *Chem. Sci.* **16**, 18976 (2025).
- [90] P. J. Flory, *Principles of polymer chemistry* (Cornell University Press, 1953).
- [91] P. G. J. van Dongen and M. H. Ernst, *Journal of Statistical Physics* **37**, 301 (1984).
- [92] J. Self, K. D. Fong, and K. A. Persson, *ACS Energy Lett.* **4**, 2843 (2019).
- [93] K. D. Fong, J. Self, K. M. Diederichsen, B. M. Wood, B. D. McCloskey, and K. A. Persson, *ACS Cent. Sci.* **5**, 2019 (1250–1260).
- [94] A. P. Thompson, H. M. Aktulga, R. Berger, D. S. Bolintineanu, W. M. Brown, P. S. Crozier, P. J. in 't Veld, A. Kohlmeyer, S. G. Moore, T. D. Nguyen, R. Shan, M. J. Stevens, J. Tranchida, C. Trott, and S. J. Plimpton, *Comp Phys Comm* **271**, 10817 (2022).
- [95] J. N. C. Lopes and A. A. Pádua, *Theoretical Chemistry Accounts* **131**, 1129 (2012).
- [96] L. Martínez, R. Andrade, E. G. Birgin, and J. M. Martínez, *J. Comput. Chem.* **30**, 2157 (2009).
- [97] G. Feng, M. Chen, S. Bi, Z. A. Goodwin, E. B. Postnikov, N. Brilliantov, M. Urbakh, and A. A. Kornyshev, *Phys. Rev. X* **9**, 021024 (2019).
- [98] D. Reber, R. Grissa, M. Becker, R.-S. Kühnel, and C. Battaglia, *Advanced Energy Materials* **11**, 2002913 (2021).
- [99] H. Cheng, Q. Sun, L. Li, Y. Zou, Y. Wang, T. Cai, F. Zhao, G. Liu, Z. Ma, W. Wahyudi, Q. Li, and J. Ming, *ACS Energy Lett.* **7**, 490 (2022).
- [100] Z. A. Goodwin, D. M. Markiewitz, Q. Wu, Y. Qi, and M. Z. Bazant, *ACS Applied Energy Materials* **8**, 8376 (2025).
- [101] R. M. Espinosa-Marzal, Z. A. Goodwin, X. Zhang, and Q. Zheng, in *One Hundred Years of Colloid Symposia: Looking Back and Looking Forward* (ACS Publications, 2023) pp. 123–148.